Have improvements in ozone air quality reduced ozone uptake into plants?

Allison C. Ronan[a], Jason A. Ducker[a], Jordan L. Schnell[b], Christopher D. Holmes[a]

[a]*Department of Earth, Ocean, and Atmospheric Science, Florida State University, Tallahassee, Florida, USA*
[b]*Department of Earth and Planetary Sciences, Northwestern University, Evanston, Illinois, USA*

*Corresponding author: cdholmes@fsu.edu

Abstract

Peak levels of ozone (O_3)—quantified by concentration metrics such as accumulated O_3 exposure over a threshold of 40 ppb (AOT40) and the sigmoidal-weighted cumulative exposure (W126)—have decreased over large parts of the United States and Europe in the last several decades. Past studies have suggested that these improvements in AOT40 and W126 indicate reductions in plant injury, even though it is widely recognized that O_3 flux into leaves, not ambient O_3 concentration, is the cause of plant damage. Using a new dataset of O_3 uptake into plants derived from eddy covariance flux towers, we test whether AOT40, W126, or summer mean O_3 are useful indicators of trends in the cumulative uptake of O_3 into leaves, which is the phytotoxic O_3 dose (POD or POD_y, where y is a detoxification threshold). At 32 sites in the United States and Europe, we find that the AOT40 and W126 concentration metrics decreased over 2005-2014 at most sites: 25 and 28 sites, respectively. POD_0, however, increased at a majority (18) of the sites. Multiple statistical tests demonstrate that none of the concentration metrics—AOT40, W126, and mean O_3—are good predictors of POD_0 temporal trends or variability ($R^2 \leq 0.15$). These results are insensitive to using a detoxification threshold (POD_3). The divergent trends for O_3 concentration and plant uptake are due to stomatal control of flux, which is shaped by environmental variability and plant factors. As a result, there has been no widespread, clear improvement in POD over 2005-2014 at the sites we can assess. Decreases in concentration metrics, therefore, give an overly optimistic and incomplete picture of the direction and magnitude of O_3 impacts on vegetation. Because of this lack of relation between O_3 flux and concentration, flux metrics should be preferred over concentration metrics in assessments of plant injury from O_3.

1. Introduction

Ground-level ozone (O_3) is harmful to people and plants (Ainsworth et al., 2012; Fleming et al., 2018). In plants, O_3 causes internal oxidative damage following uptake through their stomata, which then slows photosynthesis (Reich and Amundson, 1985; Morgan et al., 2003; Ainsworth et al., 2012), impairs stomatal control (Hoshika et al., 2015), suppresses the land-carbon sink, and indirectly forces climate change (Sitch et al., 2007; Lombardozzi et al., 2012). O_3 exposure can also increase plant metabolic costs (Iriti and Faoro, 2009), affect reproduction (Black et al., 2000; Iriti and Faoro, 2009), alter nutrient cycling and biodiversity (Fuhrer et al., 2016), heighten the effects of other environmental stressors (Sandermann et al., 1998; Black et al., 2000; Iriti and Faoro, 2009), and diminish crop yield and quality (Ainsworth, 2017). Although plant species and varieties vary in their sensitivity to O_3 (Feng et al., 2018; Harmens et al., 2018; Mills et al., 2018c), nearly all are injured to some degree and O_3 is the most damaging air pollutant for most plants (Krupa et al., 2001; Wittig et al., 2009; Ainsworth et al., 2012; Lombardozzi et al., 2012). At present-day levels of O_3, injuries are documented in crops, grasses, shrubs, and trees across Europe, North America, and Asia (Chappelka and Samuelson, 1998; Krupa et al., 2001; Baumgarten et al., 2009; Sarkar and Agrawal, 2010; Mills et al., 2011a; Ainsworth et al., 2012; Tang et al., 2013; Feng et al., 2014; Büker et al., 2015; Hoshika et al., 2015). These injuries reduce crop yields and lead to economic losses. It is estimated that O_3 has reduced global soybean, wheat, rice, and maize yields about by 5-15%, valued at $10-25 billion annually (Reich and Amundson, 1985; Van Dingenen et al., 2009; Fishman et al., 2010; Avnery et al., 2011; Tai et al., 2014; Mills et al., 2018c). The magnitude of these impacts and their relevance to food security and carbon storage in the biosphere show the importance of quantifying and understanding trends in O_3 and its impacts on vegetation, which is our goal in this work.

Several metrics are used to quantify surface O_3 and its impacts. For human health, the maximum daily average over 8 hours (MDA8), a concentration metric, is widely used to predict respiratory injury (EPA, 2011; McDonnell et al., 2012; Turner et al., 2016; Fleming et al., 2018). For assessing plant impacts, some metrics quantify O_3 concentration in ambient air while others quantify the flux of O_3 into leaf tissue through the stomata. The most widely used concentration metrics are the accumulated O_3 exposure over a threshold of 40 ppb (AOT40) and sigmoidal-weighted cumulative exposure (W126) indices, both of which give greater weight to high concentrations (Lefohn and Runeckles, 1987; Hůnová et al., 2003; Avnery et al., 2011; Lefohn et al., 2018; Mills et al., 2018a). Although correlations between these concentration metrics and plant injuries have been reported, the flux of O_3 through stomata is a better predictor of plant damage because it reflects the physiological dose to tissues within the leaves (Musselman et al., 2006; Mills et al., 2011a,b; Braun et al., 2014; Büker et al., 2015; CLRTAP, 2017). The phytotoxic O_3 dose (POD) metric integrates the stomatal flux over a growing season or other designated time period. The related POD_y metric integrates flux that exceeds a threshold (y nmol O_3 m^{-2} s^{-1}) that can be detoxified by the plant (POD_y, Mills et al., 2011a,b; CLRTAP, 2017; Mills et al., 2018a). When stomata are closed, high ambient O_3 concentrations may not injure plants. Conversely, when stomata are open wide, large fluxes and resulting injuries can occur at low O_3 concentrations. For these reasons, flux-based metrics are generally preferred, where they are available, and critical POD_y levels have been determined for many plant species (Mills et al., 2011b; CLRTAP, 2017). Indeed, several studies have found that impacts predicted from modeled stomatal uptake differ in size and pattern from impacts predicted from concentration metrics (Mills et al., 2011a; 2018c; Tang et al., 2013). Despite the advantages of POD and related flux metrics over concentration metrics, however, many plant impact studies continue to use concentration metrics because O_3 concentration data are much more widely available than stomatal O_3 flux data (Fuhrer et al., 1997; Musselman et al., 2006; Van Dingenen et al., 2009; Avnery et al., 2011; Mills et al., 2011a; Braun et al., 2014; Holmes, 2014; Lefohn et al., 2018; Mills et al., 2018a).

Across large parts of the United States and Europe, surface O_3 air quality has improved in recent decades, according to many concentration metrics (Cooper et al., 2014; Chang et al., 2017; Lefohn et al., 2017; Fleming et al., 2018; Lefohn et al., 2018; Mills et al., 2018a), after deteriorating for much of the 20th century (Vingarzan, 2004; Shindell et al., 2006; Parrish et al., 2012; Cooper et al., 2014). These recent O_3 improvements resulted from policies and technology that reduced emissions of O_3 precursors, particularly nitrogen oxides, carbon monoxide, and volatile organic compounds (EPA, 2003; Council of the European Union and European Parliament, 2008; EPA, 2011; EEA, 2016; EPA, 2016). The Tropospheric Ozone Assessment

Report (TOAR) concluded that these O_3 declines reduced the potential risk of damage to crops and other vegetation in these regions, while recognizing that climate, soil, and plant controls on stomatal conductance also determine the risk of damage (Mills et al., 2018a, hereafter TOAR-Vegetation). While the TOAR-Vegetation report used concentration metrics—principally AOT40 and W126—because long-term O_3 flux data are very sparse, the report recommended that stomatal uptake metrics be used in future risk assessments (Lefohn et al., 2018; Mills et al., 2018a).

Although some studies use empirical stomatal models to calculate O_3 flux metrics and predict reductions in crop yield (Emberson et al., 2000; Mills et al., 2011a; Büker et al., 2012; Grünhage et al., 2012; Tang et al., 2013; Emberson et al., 2013; Mills et al., 2018b, 2018c), there has been little analysis of decadal or longer trends in POD or whether those trends match the trends in concentration metrics (Colette et al., 2018). POD and concentration metrics can be well correlated, at least on short time scales, under conditions where stomatal variability is limited, such as containers with a single plant species or irrigated and fertilized fields (Cieslik, 2004; Karlsson et al., 2004; Gonzalez-Fernandez et al., 2010; Matyssek et al., 2010; González-Fernández et al., 2014). Under less controlled, natural conditions, however, weather, hydrology, and climate can drive substantial changes in conductance on time scales from minutes to years (Emberson et al., 2000; Büker et al., 2012; Keenan et al., 2013; Clifton et al., 2017). This environmental variability may disrupt the relationship between POD and O_3 concentration. The widespread and well-documented reductions in AOT40 and W126 in the United States and Europe may, therefore, misrepresent the benefits for plant health because of the influence of stomata on POD. As a result, there is a need to test whether O_3 flux into vegetation (POD) covaries with concentration metrics (AOT40 and W126) on multi-year time scales.

This paper quantifies temporal variability and trends of O_3 uptake into vegetation and compares them to variability and trends in O_3 concentration over a decade. While past work has documented that POD has low spatial correlation with AOT40 and W126 (Mills et al., 2011a; Ducker et al., 2018), we specifically test temporal trends and relationships. We use a new dataset of O_3 fluxes in the United States and Europe (Ducker et al., 2018), which covers the period 2005-2014 when previous studies documented declines in O_3 concentration metrics (Chang et al., 2017; Lefohn et al., 2017; Lefohn et al., 2018; Mills et al., 2018a). We will show that POD trends differ significantly from the concentration metrics—specifically AOT40, W126, and mean O_3—and we examine the implications of those divergent trends for vegetation health.

2. Ozone data and methods

We analyze trends in stomatal O_3 uptake and O_3 concentration in the SynFlux dataset. As described by Ducker et al. (2018), SynFlux calculates stomatal conductance and other components of O_3 deposition velocity from measurements at eddy covariance flux towers (Pastorello et al., 2017), with some additional information from remote sensing. The method uses observed fluxes of water vapor, heat, and momentum, leaf area, and standard meteorology variables. Direct measurements of O_3 flux are not needed for SynFlux. The stomatal conductance and deposition velocity are then combined with a gridded dataset of O_3 mole fractions to estimate stomatal fluxes of O_3 into vegetation around the flux tower. The O_3 dataset, described by Schnell et al. (2014), is a weighted interpolation of about 4000 of air quality monitoring stations and has horizontal resolution of 1° and temporal resolution of 1 hour. At sites with O_3 flux measurements, the gridded O_3 dataset reproduces 60-90% of observed daily O_3 variability (R^2 = 0.6–0.9) with mean bias of 5-10 ppb (Ducker et al., 2018). At a broader range of sites, Schnell et al. (2014) estimated gridded O_3 errors to be 6-9 ppb (rms). Since O_3 errors at a particular site and time affect all concentration and flux metrics simultaneously, the metric vs. metric comparisons shown here are insulated from inaccuracies in the O_3 dataset. SynFlux reproduces approximately 90% of the day-to-day variability (R^2 = 0.9) in stomatal O_3 uptake at flux measurement sites with a mean bias of 20% or less that can mostly be explained by the O_3 concentration bias (Ducker et al., 2018).

We examine trends in O_3 concentration and POD in the summer growing season over the ten-year period 2005-2014. This decade has the greatest number of sites in the SynFlux dataset and longer periods would significantly reduce the number of sites in the analysis. All SynFlux sites with at least eight years of observations in the period are used, which results in 32 qualifying sites: 10 in the United States and 22 in Europe. These sites are listed in Table S1. The sites sample ecosystem types that are widely distributed in the United States and Europe. Of the 32 sites, 21 are forests (10 needleleaf, 7 broadleaf, and 4 mixed), 5 are grassland, 2 are crops, 2 are savanna or shrubland, and 1 is wetland.

At each SynFlux site, we calculate POD_0, POD_3, AOT40, W126, and daytime mean O_3 for each summer growing season, defined as June-September. POD_y is the cumulative daytime stomatal flux above threshold y nmol m^{-2} s^{-1} during these months, which is contained in the SynFlux dataset described by Ducker et al. (2018). Recommended thresholds vary by species, so we use POD_3, a predictor for damage in several vegetation types (Mills et al., 2011a; Büker et al., 2015; CLRTAP, 2017), to test whether the threshold affects our results. We integrate the stomatal flux over times when the sun is at least four degrees above the horizon. When some stomatal flux data are missing, the integral of available fluxes in each month is scaled up by the fraction of missing data; the scaled monthly integrals are summed to obtain POD_y for the summer growing season. Months with fewer than 100 observations are discarded from the analysis because of the greater uncertainty in the monthly integral. When one of the four growing season months is missing, we scale up the remaining months in the same way to get total POD_y for the growing season; if two or more months are missing, the POD_y is treated as missing for that year. The AOT40 and W126 metrics are calculated from the gridded O_3 dataset following previously documented methods (Ducker et al., 2018; Lefohn et al., 2018). Unlike some studies, we do not apply a three-year running mean, so our W126 and AOT40 values describe O_3 concentrations in the summer growing season of a single year. Gaps in the O_3 concentration data, although rare, are treated similarly to POD_y, by scaling up the AOT40 or W126 by the fraction of missing data. All metrics are calculated over the same growing period, June-September, at all 32 sites. Accumulating the O_3 metrics over site-specific growing months could alter the metric values or their trends, but is less likely to affect whether POD_y and concentration metrics have consistent temporal variability, which is the main focus of this work. In cases where POD_y is missing for a particular site and year, the AOT40, W126, and mean O_3 are also discarded for consistent analysis of trends and variability. For some analyses, we remove mean spatial differences between sites by computing anomalies, $x - \bar{x}$, where x represents a metric value at a particular site and $\bar{x}$ is its 10-year mean at that site. To compare fractional changes among metrics with different units, we also normalize values using $x' = x/\bar{x} - 1$. Figure S1 shows time series of all normalized metrics.

We estimate the linear trends in O_3 metrics at each site using ordinary least squares regression: $x = a + bt$, where x represents a metric value, t is time, and a and b are fitted parameters. To test if two metrics have the same trend, we normalize the metrics, as described above, and add interaction effects to the regression model: $x' = a + bt + \alpha C + \beta C t$, where C is a categorical variable for metric type ($C = 0$ for metric one, $C = 1$ for metric two) and α and β are fitted parameters expressing the differences in the intercept and slope, respectively, for the two metrics. If β is significantly different from zero, then the metrics have different trends. We will use this approach to compare pairwise the trends in POD_0, POD_3, AOT40, and W126, thus highlighting the relationship between the flux and concentration metrics. In addition to standard p-values of regression coefficients, we use Fisher's combined probability test, a meta-analysis method, to assess whether an ensemble of p-values collectively provide evidence of an effect (Fisher, 1934). We also assess the temporal co-variability of metrics in three additional ways. First, we pool the anomaly data from all sites and years ($n = 299$) and compute the coefficient of determination (R^2) for each pair of metrics. Any correlation among the anomalies is strictly from temporal co-variability since mean spatial differences have been removed. Second, we calculate the coefficients of determination site-by-site for each pair of metrics (m = 8-10 years) and then average the resulting R^2 values across sites ($n = 32$). Finally, we correlate the temporal trends, described above, for each pair of metrics ($n = 32$ sites). Analyses are performed in Python using the statsmodels module for statistical tests (Seabold and Perktold, 2010). We use the graphical format of Cooper et al. (2014) and Mills et al. (2018a) to visualize trend results in Figures 1 and 2.

3. Trends in O_3 uptake and concentration metrics

Figures 1 and 2 show that summer daytime mean O_3 concentrations decreased at a large majority of sites over 2005-2014—14 of the 22 European SynFlux sites and 7 of the 10 sites in the United States—although only 3 sites had trends with the customary $p < 0.05$ level. Past studies have found that the highest quantiles of O_3 distribution have fallen faster than the median and lower quantiles (Cooper et al., 2014; Lefohn et al., 2018). As a result, W126 and AOT40, which emphasize high concentrations, have stronger declining trends than daytime mean O_3. For W126, 28 of the 32 sites have negative trends and 7 of these have $p < 0.05$. For AOT40, 25 of the 32 sites have decreasing trends and 3 have $p < 0.05$. No sites had positive trends with $p < 0.05$ for either AOT40 or W126.

Our analysis methods differ from some past trend studies in that we use gridded O_3 data rather than original station measurements. Nevertheless, our concentration trend patterns are very similar to those reported by others (Cooper et al., 2014; Lefohn et al., 2017; Mills et al., 2018a), despite each of those studies using different averaging methods (daytime or 24 hour) and examining different ranges of years. They generally show that summer mean O_3 in Europe has decreased or held steady since the 1990s, while concentrations in the United States decreased in the eastern United States and were steady or rising across most of the western and central United States. Like us, those earlier studies also found more consistent downward trends in AOT40 and W126 than mean O_3 in all of these regions except the western and central United States (Fleming et al., 2018; Mills et al., 2018a). The TOAR-Vegetation analysis suggests that statistically significant declines of W126 and AOT40 are more widespread than we report (45-50% of TOAR-Vegetation sites in the United States and Europe had declines; Mills et al., 2018a), but this apparent difference is explained by the larger fraction of TOAR-Vegetation sites in areas recovering from severe historical O_3 pollution, like the eastern United States and California, and the longer period of the TOAR-Vegetation analysis (1995-2014). Overall, the comparison shows that our trend results for concentration metrics using SynFlux and gridded O_3 fields are consistent with TOAR-Vegetation results using station O_3 observations.

Trends in POD_0 are distinctly different from trends in mean O_3, AOT40, and W126, as seen in Figures 1, 2, and S1. Unlike all of the concentration metrics, POD_0 increased at more than half (18 of 32) of the sites, although 4 had POD_0 declines with $p < 0.05$. The sign or direction of the POD_0 (and POD_3) trends also disagree with the concentration trends about as often as they agree. Of the 28 sites with decreasing W126, 16 have increasing POD_0. Of the 25 sites with decreasing AOT40, 14 have increasing POD_0. Similar patterns appear in the multi-site mean trends. For AOT40, W126, and mean O_3 the multi-site mean trends are downward ($p = 0.001$, $p \leq 0.0001$, and $p = 0.06$, respectively) while the mean POD_0 trend is upward ($p = 0.9$).

The discrepancies between POD_0 and concentration trends occur in nearly all vegetation types examined. The POD_0 trends have opposite sign to W126 and AOT trends at roughly half of the forest sites (5 of 10 needleleaf, 4 of 7 broadleaf, 3 of 4 mixed forest), grassland sites (2 of 5 sites), and shrubland sites (1 of 2). At the one wetland site all metrics have the same trend sign, which is consistent with stomatal flux correlating with O_3 concentration in a moisture-rich environment that promotes stomatal opening (CLRTAP, 2017). Conversely, at both crop sites, POD_0 and concentration trends have opposite sign. While the crop sites used irrigation, which relieves water stress, they also rotated crops in some years, which would increase the interannual variability in stomatal conductance and POD_0 while having less effect on O_3 concentrations, thereby partly decoupling O_3 concentration and uptake. Trend disagreements also occur across most of the examined geographical region and climate types, with no clear pattern. While the small number of sites for some vegetation types (particularly non-forests), regions, and climates make it difficult to determine if O_3 concentration and flux preferentially decouple in certain environments, it is clear that discrepancies between POD_y and concentration trends are widespread.

Some differences in trends should be expected because of statistical fitting errors in each slope estimate stemming from errors and uncertainty in the measurements that underlie each metric. Nevertheless, if stomatal conductance and deposition velocity were steady, the normalized O_3 concentration and normalized POD should have similar trends. Using a regression model of normalized data with interaction effects (Section 2), we find that the fractional trends in POD are indeed different ($p < 0.05$ level) from the fractional trends in other metrics at 7 sites, regardless of which concentration metric is chosen. Many more sites have trend differences with marginal or low significance ($0.05 < p < 0.2$) (9 for AOT40 and mean O_3, 11 for W126). The statistical strength of these results may be underestimated due to the random errors in SynFlux (section 2), which inflate the POD_0 variance and diminish the significance (p value) of differences from concentration metrics. Mean biases do not affect the POD_0 trends, so they should not affect the relationship to concentration metrics. In an aggregate meta-analysis (Fisher's combined probability test), the skew towards zero of all 32 p-values gives strong evidence that the normalized POD_0 trends systematically differ from the concentration trends ($p \ll 0.001$), for all normalized concentration metrics. The divergent trends for POD_0 and concentration metrics are likely explained through stomatal conductance, which is driven by many factors such as weather, hydrology, and climate. Rising stomatal conductance increases O_3 uptake into plants, while decreasing ambient O_3 concentration through dry deposition (Solberg et al., 2008; Emberson et al., 2013; Kavassalis and Murphy, 2017). Regardless of the causes, however, the divergent trends indicate that the common AOT40 and W126 metrics have limited utility for tracking changes in O_3 impacts on vegetation.

While the O_3 trends in our 10-year study period are consistent with past studies that investigated other periods, as shown above, the trends for any given site and metric can vary depending on which years are analyzed. Individual years with extreme or missing data can sometimes discernably affect trend estimates, which may contribute to a few apparently large differences between some neighboring sites (e.g. POD_0 trends in Italy). Calculating trends over a longer time period could reduce the influence of individual years, but at the expense of having fewer sites in this analysis. However, the occurrence of an extreme value in one metric but not another (e.g. W126 vs. POD_y) at a single site is still a meaningful indicator that those metrics have different temporal variability. In addition, the regression model that tests differences in trends between metrics accounts for the greater uncertainty in the individual trends that result from extreme values, yet we still find statistically significant different trends across metrics.

Another measure of the usefulness of concentration metrics is their temporal correlation with POD, shown Figures 3 and 4 and Table S2. Mills et al. (2011a) recognized that the spatial pattern of POD can be quite different from the O_3 concentration pattern, particularly when considering sites with contrasting climate and vegetation. Ducker et al. (2018) further showed that their spatial correlations are very low ($R^2 \leq 0.05$ for POD_0 vs. AOT40, W126, or mean O_3). We quantify the temporal correlation between POD_y and other metrics in three ways (Table S2). The first approach, seen in Figure 3, which pools data from all sites, reveals no meaningful correlation between POD_0 and any of the concentration metrics ($R^2 < 0.01$) while all pairs of concentration metrics are strongly correlated ($R^2 = 0.7$–0.9). Results are unchanged when using POD_3 in place of POD_0 ($R^2 < 0.01$, Figure S2). The second, site-by-site approach also shows that the concentration metrics are closely correlated with each other ($R^2 = 0.72$–0.84 averaged across sites; Table S2) but not with POD_0 ($R^2 = 0.13$-0.14). Both of these approaches mean that none of the concentration metrics can predict well the interannual variability of POD_0. Finally, the linear trends shown in Figure 4, which are fitted to data at each individual site, indicate that POD_0 trends are essentially unrelated to trends in any concentration metric ($R^2 \leq 0.05$; Figure 4; Table S2), while all of the concentration metric trends have considerable common variability ($R^2 = 0.5$–0.9). The trend correlations are again similarly weak when using POD_3 ($R^2 \leq 0.1$; Figure S3). This means that neither AOT40 trend nor W126 trend has any skill in predicting the POD_y trend.

While it is already widely recognized that variations in stomatal conductance complicate the relationship between O_3 concentrations and stomatal uptake (Musselman et al., 2006), these results go a step further. Our results show that the conductance changes under common environmental conditions are sufficiently large and important that W126 and AOT40 trends are poor predictors of POD_y trends. AOT40 and W126 might still be useful for assessing ozone extremes for other applications, however. Thus, the widespread decreases of W126 and AOT40 in large parts of the United States and Europe, while favorable, are not robust indicators for improved plant uptake or health. In fact, we have shown that there has been no widespread improvement in POD_y at sites in these regions.

4. Conclusions

By many metrics, O_3 air quality has improved in large parts of the United States and Europe over the last two decades in response to policies and technological improvements that reduced emissions of O_3 precursors. Past work and our results show that there are downward trends in mean O_3, AOT40, and W126 metrics at a majority of sites that we studied in the eastern United States and Europe. These metrics are widely used to assess the impacts of O_3 and their declines have been interpreted as indicating reduced O_3 damage to vegetation. While POD is known to be a better predictor of the physiological O_3 dose than ambient O_3 concentration, its use has been limited by data availability.

We use the SynFlux dataset to report decadal trends in POD for the first time and find that POD does not follow the same trends as the O_3 concentration metrics commonly used to assess vegetation injury. POD trends have mixed increases and decreases across the United States and Europe, in contrast to the predominant decrease in concentration metrics at the sites we examined. Many sites have simultaneous decreasing AOT40 and W126 while POD is increasing. Using multiple statistical approaches, we show that the multi-year trends and temporal variability in POD differ significantly and systematically from the concentration metrics. The results are not affected by POD_y threshold choices ($y = 0$ or 3 nmol m^{-2} s^{-1}). Past work showed that concentration metrics have low spatial correlation with POD and, here, we add that there is also little temporal correspondence. Thus, AOT40 and W126 are not robust predictors of trends in plant injuries from O_3. Rather, the widespread decreases of AOT40 and W126 in the United States and Europe in recent decades give an overly optimistic view of changing plant injury risk in recent years. If all else were equal, reduced concentrations would lead to less plant injury, but, in reality, stomatal conductance and its variability—driven by meteorology, hydrology, and climate—is an equally important control on POD. The analysis here further supports the recommendations of TOAR-Vegetation and others that future studies of plant damage and economic losses should avoid relying primarily on AOT40 or W126 and make greater effort to account for stomatal activity and stomatal flux. This is particularly important when considering the combined effects of climate variability and change in combination with evolving surface O_3 concentrations.

Competing interests

The authors have no competing interests to declare.

Author contributions

Contributed to conception and design: ACR, CDH
Contributed to acquisition of data: JAD, JLS
Contributed to analysis and interpretation of data: ACR, CDH
Drafted or revised the article: all
Approved the submitted version for publication: all

Funding information

This work was supported by the Winchester Fund at Florida State University, NASA New Investigator Program grant NNX16AI57G, and NSF CAREER grant 1848372.

Data accessibility statement

SynFlux data, including O_3 concentrations are archived and publicly available at https://doi.org/10.5281/zenodo.1402054 (Ducker et al., 2018)

References

Ainsworth EA. 2017. Understanding and improving global crop response to ozone pollution. *Plant J* **90**: 886–897. doi: 10.1111/tpj.13298

Ainsworth EA, Yendrek CR, Sitch S, Collins WJ, Emberson LD. 2012. The effects of tropospheric ozone on net primary productivity and Implications for climate change. *Annu Rev Plant Biol* **63**(1): 637–661. doi: 10.1146/annurev-arplant-042110-103829

Avnery S, Mauzerall DL, Liu J, Horowitz LW. 2011. Global crop yield reductions due to surface ozone exposure: 1. Year 2000 crop production losses and economic damage. *Atmos Environ* **45**: 2284–2296. doi: 10.1016/j.atmosenv.2010.11.045

Baumgarten M, Huber C, Büker P, Emberson L, Dietrich HP, Nunn AJ, Heerdt C, Beudert B, Matyssek R. 2009. Are Bavarian Forests (southern Germany) at risk from ground-level ozone? Assessment using exposure and flux based ozone indices. *Environ Pollut* **157**: 2091–2107. doi: 10.1016/j.envpol.2009.02.012

Black VJ, Black CR, Roberts JA, Stewart CA. 2000. Impact of ozone on the reproductive development of plants. *New Phytol* **147**(3): 421–447. doi: 10.1046/j.1469-8137.2000.00721.x

Braun S, Schindler C, Rihm B. 2014. Growth losses in Swiss forests caused by ozone: Epidemiological data analysis of stem increment of Fagus sylvatica L. and Picea abies Karst. *Environ Pollut* **192**: 129–138. doi: 10.1016/j.envpol.2014.05.016

Büker P, Feng Z, Uddling J, Briolat A, Alonso R, Braun S, Elvira S, Gerosa G, Karlsson PE, Le Thiec D, et al. 2015. New flux based dose-response relationships for ozone for European forest tree species. *Environ Pollut* **206**: 163–174. doi: 10.1016/j.envpol.2015.06.033

Büker P, Morrissey T, Briolat A, Falk R, Simpson D, Tuovinen JP, Alonso R, Barth S, Baumgarten M, Grulke N, et al. 2012. DO3SE modelling of soil moisture to determine ozone flux to forest trees. *Atmos Chem Phys* **12**: 5537–5562. doi: 10.5194/acp-12-5537-2012

Chang K-L, Petropavlovskikh I, Copper OR, Schultz MG, Wang T. 2017. Regional trend analysis of surface ozone observations from monitoring networks in eastern North America, Europe and East Asia. *Elem Sci Anth* **5**: 50. doi: 10.1525/elementa.243

Chappelka AH, Samuelson LJ. 1998. Ambient ozone effects on forest trees of the eastern United States. *New Phytol* **139**: 91–108.

Cieslik SA. 2004. Ozone uptake by various surface types: A comparison between dose and exposure. *Atmos Environ* **38**: 2409–2420. doi: 10.1016/j.atmosenv.2003.10.063

Clifton OE, Fiore AM, Munger JW, Malyshev S, Horowitz LW, Shevliakova E, Paulot F, Murray LT, Griffin KL. 2017. Interranual variability in ozone removal by a temperate deciduous forest. *Geophsyical Res Lett*: 542–552. doi: 10.1002/2016GL070923

CLRTAP. 2017. Mapping critical levels for vegetation, revised Chapter 3 of the Manual on Methodologies and Criteria for Modelling and Mapping Critical Loads and Levels and Air Pollution Effects, Risks and Trends. United National Economic Commission for Europe (UNECE). Convention on Long-range Transboundary Air Pollution (CLRTAP).

Colette A, Tognet F, Létinois L, Lemaire V, Couvidat F, Alonso Del Amo RM, Gonzalez Fernandez IA, Rábago Juan-Aracil I, Harmens H, Andersson C, et al. 2018. *ETC/ACM Report 2018:15: Long-Term Evolution of the Impacts of Ozone Air Pollution on Agricultural Yields in Europe*. Bilthoven: European Topic Centre on Air Pollution and Climate Change Mitigation

Cooper OR, Parrish DD, Ziemke J, Balashov N V., Cupeiro M, Galbally IE, Gilge S, Horowitz

L, Jensen NR, Lamarque J-F, et al. 2014. Global distribution and trends of tropospheric ozone: An observation-based review. *Elem Sci Anthr* **2**: 1–28. doi: 10.12952/journal.elementa.000029
Council of the European Union, European Parliament. 2008. Directive 2008/50/EC of the European Parliament and of the Council of 21 May 2008 on ambient air quality and cleaner air for Europe. *Off J Eur Union* **L152**: 1–44. Available at https://eur-lex.europa.eu/eli/dir/2008/50/oj.
Ducker JA, Holmes CD, Keenan TF, Fares S, Goldstein AH, Mammarella I, William Munger J, Schnell J. 2018. Synthetic ozone deposition and stomatal uptake at flux tower sites. *Biogeosciences* **15**(17): 5395–5413. doi: 10.5194/bg-15-5395-2018
EEA. 2016. Air quality in Europe — 2016 report. European Environment Agency. doi: 10.2800/80982
Emberson LD, Ashmore MR, Cambridge HM, Simpson D, Tuovinen JP. 2000. Modelling stomatal ozone flux across Europe. *Environ Pollut* **109**: 403–413. doi: 10.1016/S0269-7491(00)00043-9
Emberson LD, Kiwiroon N, Beevers S, Büker P, Cinderby S. 2013. Scorched Earth : how will changes in the strength of the vegetation sink to ozone deposition affect human health and ecosystems? *Atmos Chem Phys* **13**: 6741–6755. doi: 10.5194/acp-13-6741-2013
EPA. 2003. Ozone Transport Commission NOx Budget Program 1999-2002 Progress Report. United States Environmental Protection Agency.
EPA. 2011. EPA's NOx Reduction Program and Clean Air Interstate Rule: 2009 Environmental and Health Results. United States Environmental Protection Agency. Available at https://www.epa.gov/sites/production/files/2015-08/documents/cair09_environmental_results.pdf
EPA. 2016. Air Pollutant Emissions Trends Data. State Average Annual Emissions Trend. United States Environmental Protection Agency. Available at https://www.epa.gov/air-emissions-inventories/air-pollutant-emissions-trends-data.
Feng Z, Büker P, Pleijel H, Emberson L, Karlsson PE, Uddling J. 2018. A unifying explanation for variation in ozone sensitivity among woody plants. *Glob Chang Biol* **24**(1): 78–84. doi: 10.1111/gcb.13824
Feng Z, Sun J, Wan W, Hu E, Calatayud V. 2014. Evidence of widespread ozone-induced visible injury on plants in Beijing, China. *Environ Pollut* **193**: 296–301. doi: 10.1016/j.envpol.2014.06.004
Fisher RA. 1934. The combination of probabilities from tests of significance. In: *Statistical Methods for Research Workers,* 5th ed. Edinburgh: Oliver and Boyd.
Fishman J, Creilson JK, Parker PA, Ainsworth EA, Vining GG, Szarka J, Booker FL, Xu X. 2010. An investigation of widespread ozone damage to the soybean crop in the upper Midwest determined from ground-based and satellite measurements. *Atmos Environ* **44**: 2248–2256. doi: 10.1016/j.atmosenv.2010.01.015
Fleming ZL, Doherty RM, Von Schneidemesser E, Malley CS, Cooper OR, Pinto JP, Colette A, Xu X, Simpson D, Schultz MG, et al. 2018. Tropospheric Ozone Assessment Report: Present-day ozone distribution and trends relevant to human health. *Elem Sci Anth* **6**(1): 12. doi: 10.1525/elementa.273
Fuhrer J, Skärby L, Ashmore MR. 1997. Critical levels for ozone effects on vegetation in Europe. *Environ Pollut* **97**(1–2): 91–106. doi: 10.1016/S0269-7491(97)00067-5
Fuhrer J, Val Martin M, Mills G, Heald CL, Harmens H, Hayes F, Sharps K, Bender J, Ashmore

MR. 2016. Current and future ozone risks to global terrestrial biodiversity and ecosystem processes. *Ecol Evol* **6**(24): 8785–8799. doi: 10.1002/ece3.2568

González-Fernández I, Calvo E, Gerosa G, Bermejo V, Marzuoli R, Calatayud V, Alonso R. 2014. Setting ozone critical levels for protecting horticultural Mediterranean crops: Case study of tomato. *Environ Pollut* **185**: 178–187. doi: 10.1016/j.envpol.2013.10.033

Gonzalez-Fernandez I, Kaminska A, Dodmani M, Goumenaki E, Quarrie S, Barnes JD. 2010. Establishing ozone flux-response relationships for winter wheat: Analysis of uncertainties based on data for UK and Polish genotypes. *Atmos Environ* **44**: 621–630. doi: 10.1016/j.atmosenv.2009.11.021

Grünhage L, Pleijel H, Mills G, Bender J, Danielsson H, Lehmann Y, Castell JF, Bethenod O. 2012. Updated stomatal flux and flux-effect models for wheat for quantifying effects of ozone on grain yield, grain mass and protein yield. *Environ Pollut* **165**: 147–157. doi: 10.1016/j.envpol.2012.02.026

Harmens H, Hayes F, Mills G, Sharps K, Osborne S, Pleijel H. 2018. Wheat yield responses to stomatal uptake of ozone: Peak vs rising background ozone conditions. *Atmos Environ* **173**(January): 1–5.

Holmes CD. 2014. Air pollution and forest water use. *Nature* **507**(7491): E1–E2. doi: 10.1038/nature13113

Hoshika Y, Katata G, Deushi M, Watanabe M, Koike T, Paoletti E. 2015. Ozone-induced stomatal sluggishness changes carbon and water balance of temperate deciduous forests. *Sci Rep* **5**(May): 1–8. doi: 10.1038/srep09871

Hůnová I, Livorová H, Ostatnická J. 2003. Potential ambient ozone impact on ecosystems in the Czech Republic as indicated by exposure index AOT40. *Ecol Indic* **3**: 35–47. doi: 10.1016/S1470-160X(03)00009-8

Iriti M, Faoro F. 2009. Chemical diversity and defence metabolism: How plants cope with pathogens and ozone pollution. *Int J Mol Sci* **10**(8): 3371–3399. doi: 10.3390/ijms10083371

Karlsson PE, Uddling J, Braun S, Broadmeadow M, Elvira S, Gimeno BS, Le Thiec D, Oksanen E, Vandermeiren K, Wilkinson M, et al. 2004. New critical levels for ozone effects on young trees based on AOT40 and simulated cumulative leaf uptake of ozone. *Atmos Environ* **38**: 2283–2294. doi: 10.1016/j.atmosenv.2004.01.027

Kavassalis SC, Murphy JG. 2017. Understanding ozone-meteorology correlations: A role for dry deposition. *Geophys Res Lett* **44**(6): 2922–2931. doi: 10.1175/JCLI-D-12-00168.1

Keenan TF, Hollinger DY, Bohrer G, Dragoni D, Munger JW, Schmid HP, Richardson AD. 2013. Increase in forest water-use efficiency as atmospheric carbon dioxide concentrations rise. *Nature* **499**: 324–327. doi: 10.1038/nature12291

Krupa S, Mcgrath MT, Andersen CP, Booker FL, Burkey KO, Chappelka AH, Chevone BI, Pell EJ, Zilinskas B a. 2001. Ambient ozone and plant health. *Plant Dis* **85**(1): 4–12. doi: 10.1094/PDIS.2001.85.1.4

Lefohn AS, Malley CS, Simon H, Wells B, Xu X, Zhang L, Wang T. 2017. Responses of human health and vegetation exposure metrics to changes in ozone concentration distributions in the European Union, United States, and China. *Atmos Environ* **152**: 123–145. doi: 10.1016/j.atmosenv.2016.12.025

Lefohn AS, Malley CS, Smith L, Wells B, Hazucha M, Simon H, Naik V, Mills G, Schultz MG, Paoletti E, et al. 2018. Tropospheric ozone assessment report: Global ozone metrics for climate change, human health, and crop/ecosystem research. *Elem Sci Anthr* **6**: 28. doi: 10.1525/elementa.279

Lefohn AS, Runeckles VC. 1987. Establishing standards to protect vegetation-ozone exposure/dose considerations. *Atmos Environ* **21**: 561–568. doi: 10.1016/0004-6981(87)90038-2

Lombardozzi D, Sparks JP, Bonan G, Levis S. 2012. Ozone exposure causes a decoupling of conductance and photosynthesis: implications for the Ball-Berry stomatal conductance model. *Oecologia* **169**: 651–659. doi: 10.1007/s00442-011-2242-3

Matyssek R, Karnosky DF, Wieser G, Percy K, Oksanen E, Grams TEE, Kubiske M, Hanke D, Pretzsch H. 2010. Advances in understanding ozone impact on forest trees: messages from novel phytotron and free-air fumigation studies. *Environ Pollut* **158**(6): 1990–2006. doi: 10.1016/j.envpol.2009.11.033

McDonnell WF, Stewart PW, Smith M V., Kim CS, Schelegle ES. 2012. Prediction of lung function response for populations exposed to a wide range of ozone conditions. *Inhal Toxicol* **24**(10): 619–633. doi: 10.3109/08958378.2012.705919

Mills G, Hayes F, Simpson D, Emberson L, Norris D, Harmens H, Büker P. 2011a. Evidence of widespread effects of ozone on crops and (semi-)natural vegetation in Europe (1990-2006) in relation to AOT40- and flux-based risk maps. *Glob Chang Biol* **17**: 592–613. doi: 10.1111/j.1365-2486.2010.02217.x

Mills G, Pleijel H, Braun S, Büker P, Bermejo V, Danielsson H, Emberson L, Grünhage L, González-Fernández I, Harmens H, Hayes F, Karlsson PE, Simpson D. 2011b. New stomatal flux-based critical levels for ozone effects on vegetation. *Atmos Environ* **45**: 5064 – 5068. doi: 10.1016/j.atmosenv.2011.06.009

Mills G, Pleijel H, Malley CS, Sinha B, Cooper OR, Schultz MG, Neufeld HS, Simpson D, Sharps K, Feng Z, et al. 2018a. Tropospheric Ozone Assessment Report: present-day ozone distribution and trends relevant to vegetation. *Elem Sci Anthr* **6**(47): 46. doi: 10.1525/elementa.302

Mills, G, Sharps, K, Simpson, D, Pleijel, H, Broberg, M, Uddling, J, Jaramillo, F, Davies, W J, Dentener, F, Van den Berg, M, et al. 2018b. Ozone pollution will compromise efforts to increase global wheat production. *Glob Change Biol* **24:** 3560 – 3574. doi:10.1111/gcb.14157

Mills, G, Sharps, K, Simpson, D, Pleijel, H, Frei, M, Burkey, K, Emberson, L, Uddling, J, Broberg, M, Feng, Z, et al. 2018c. Closing the global ozone yield gap: Quantification and cobenefits for multistress tolerance. *Glob Chang Biol* **24**(10): 4869–4893. doi: 10.1111/gcb.14381

Morgan PB, Ainsworth EA, Long SP. 2003. How does elevated ozone impact soybean? A meta-analysis of photosynthesis, growth and yield. *Plant, Cell Environ* **26**(8): 1317–1328. doi: 10.1046/j.0016-8025.2003.01056.x

Musselman RC, Lefohn AS, Massman WJ, Heath RL. 2006. A critical review and analysis of the use of exposure- and flux-based ozone indices for predicting vegetation effects. *Atmos Environ* **40**: 1869–1888. doi: 10.1016/j.atmosenv.2005.10.064

Parrish DD, Law KS, Staehelin J, Derwent R, Cooper OR, Tanimoto H, Gilge S. 2012. and Physics Long-term changes in lower tropospheric baseline ozone concentrations at northern mid-latitudes. *Atmos Chem Phys*: 11485–11504. doi: 10.5194/acp-12-11485-2012

Pastorello GZ, Papale D, Chu H, Trotta C, Agarwal DA, Canfora E, Baldocchi DD. 2017. A new data set to keep a sharper eye on land-air exchanges. *Eos* **98**: 28–32. doi: 10.1029/2017EO071597

Reich PB, Amundson RG. 1985. Ambient levels of ozone reduce net photosynthesis in tree and crop species. *Am Assoc Adv Sci* **230**(4725): 566–570. doi: 10.1126/science.230.4725.566

Sandermann H, Ernst D, Heller W, Langebartels C. 1998. Ozone: An abiotic elicitor of plant defence reactions. *Trends Plant Sci* **3**(2): 47–50. doi: 10.1016/S1360-1385(97)01162-X

Sarkar A, Agrawal SB. 2010. Identification of ozone stress in Indian rice through foliar injury and differential protein profile. *Environ Monit Assess* **161**: 205–215. doi: 10.1007/s10661-008-0738-z

Schnell JL, Holmes CD, Jangam A, Prather MJ. 2014. Skill in forecasting extreme ozone pollution episodes with a global atmospheric chemistry model. *Atmos Chem Phys* **14**: 7721–7739. doi: 10.5194/acp-14-7721-2014

Seabold S, Perktold J. 2010. Statsmodels: econometric and statistical modeling with Python. *Proceedings of the 9th Python in Science Conference* (SciPy 2010): 57–61. Available at http://conference.scipy.org/proceedings/scipy2010/pdfs/seabold.pdf.

Shindell D, Faluvegi G, Lacis A, Hansen J, Ruedy R, Aguilar E. 2006. Role of tropospheric ozone increases in 20th-century climate change. *J Geophys Res* **111**: 1–11. doi: 10.1029/2005JD006348

Sitch S, Cox PM, Collins WJ, Huntingford C. 2007. Indirect radiative forcing of climate change through ozone effects on the land-carbon sink. *Nature* **448**: 791–794. doi: 10.1038/nature06059

Solberg S, Hov O, Sovde A, Isaksen ISA, Coddeville P, De Backer H, Forster C, Orsolini Y, Uhse K. 2008. European surface ozone in the extreme summer 2003. *J Geophys Res* **113**(D7): D07307. doi: 10.1029/2007JD009098

Tai APK, Martin MV, Heald CL. 2014. Threat to future global food security from climate change and ozone air pollution. *Nature Climate Change* **4**(9): 817–821. doi: 10.1038/nclimate2317

Tang H, Takigawa M, Liu G, Zhu J, Kobayashi K. 2013. A projection of ozone-induced wheat production loss in China and India for the years 2000 and 2020 with exposure-based and flux-based approaches. *Glob Chang Biol* **19**: 2739–2752. doi: 10.1111/gcb.12252

Turner MC, Jerrett M, Pope CA, Krewski D, Gapstur SM, Diver WR, Beckerman BS, Marshall JD, Su J, Crouse DL, et al. 2016. Long-term ozone exposure and mortality in a large prospective study. *Am J Respir Crit Care Med* **193**(10): 1134–1142. doi: 10.1164/rccm.201508-1633OC

Van Dingenen R, Dentener FJ, Raes F, Krol MC, Emberson L, Cofala J. 2009. The global impact of ozone on agricultural crop yields under current and future air quality legislation. *Atmos Environ* **43**: 604–618. doi: 10.1016/j.atmosenv.2008.10.033

Vingarzan R. 2004. A review of surface ozone background levels and trends. *Atmos Environ* **38**: 3431–3442. doi: 10.1016/j.atmosenv.2004.03.030

Wittig VE, Ainsworth EA, Naidu SL, Karnosky DF, Long SP. 2009. Quantifying the impact of current and future tropospheric ozone on tree biomass, growth, physiology and biochemistry: a quantitative meta-analysis. *Glob Chang Biol* **15**: 396–424. doi: 10.1111/j.1365-2486.2008.01774.x

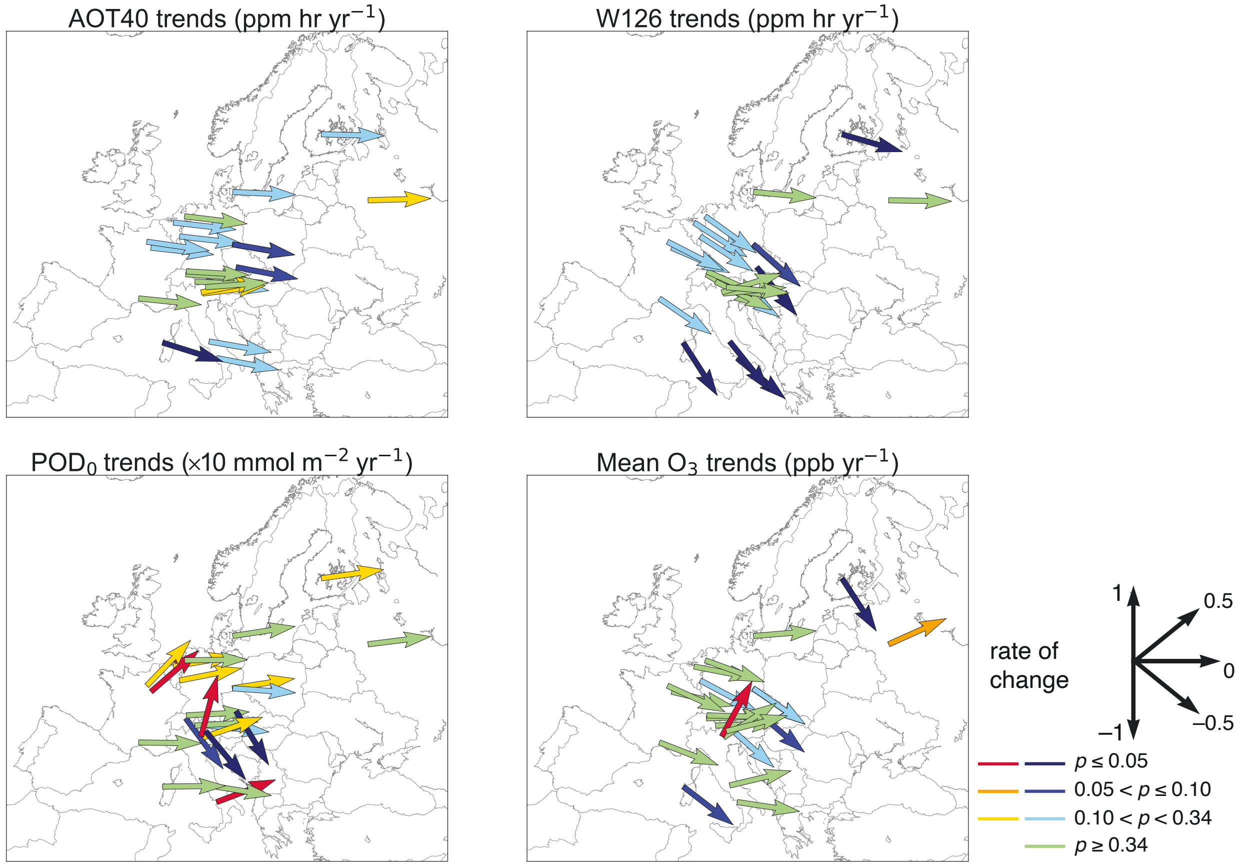

Figure 1. Trends (2005-2014) in O_3 metrics relevant to plant injury at SynFlux sites in Europe. All metrics are calculated for June-September daytime. Arrows show linear trends and colors indicate significance of the trend (*p* value).

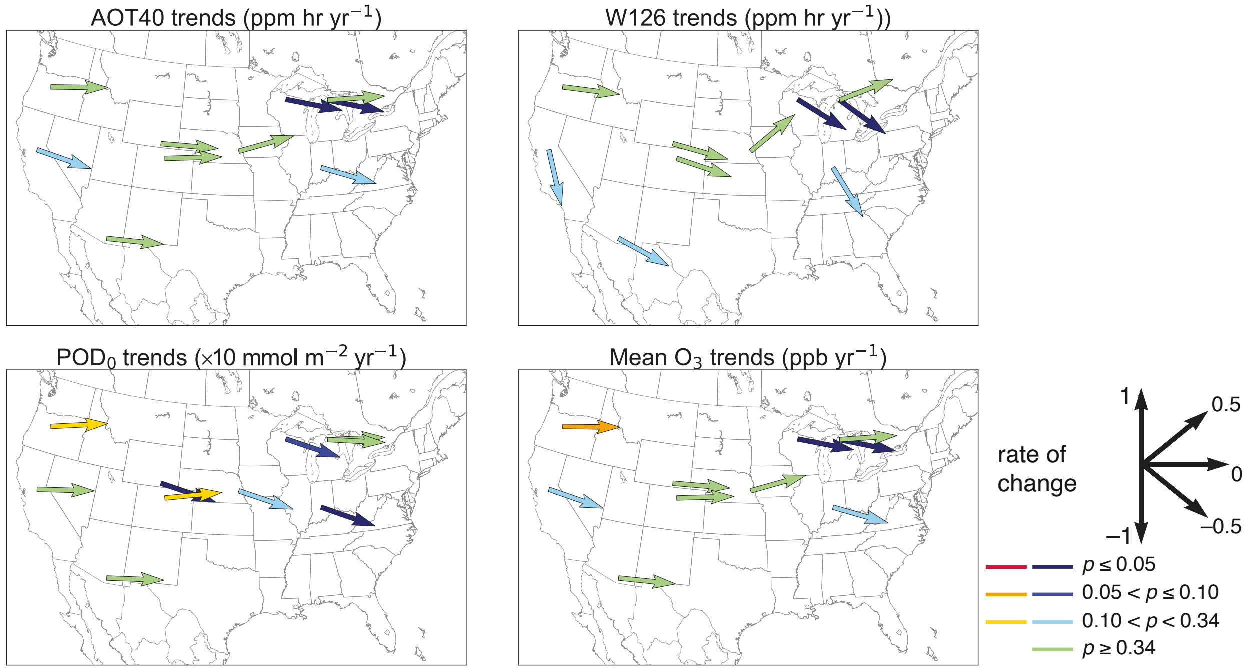

Figure 2. Trends (2005-2014) in O_3 metrics relevant to plant injury at SynFlux sites in the United States. See Figure 1 caption.

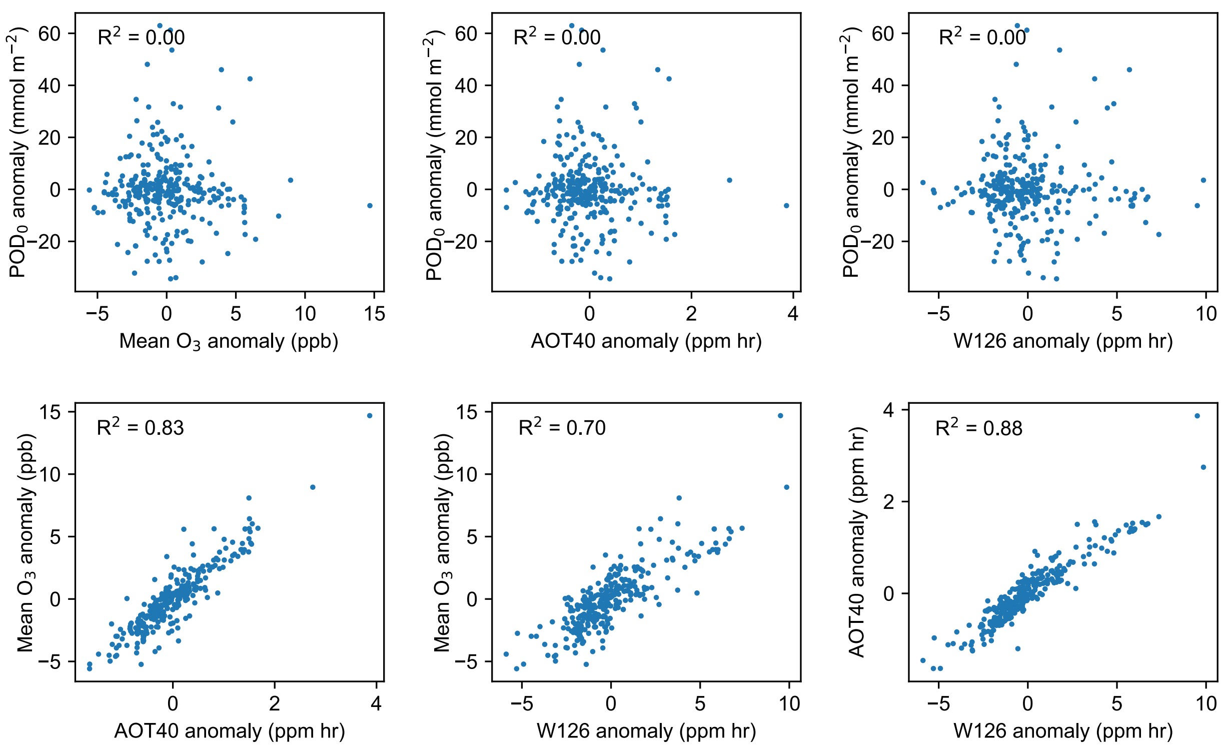

Figure 3. Temporal co-variation of ozone metrics relevant to vegetation health. Each point represents a single site and year. The site-specific mean has been subtracted from each metric to highlight temporal co-variability.

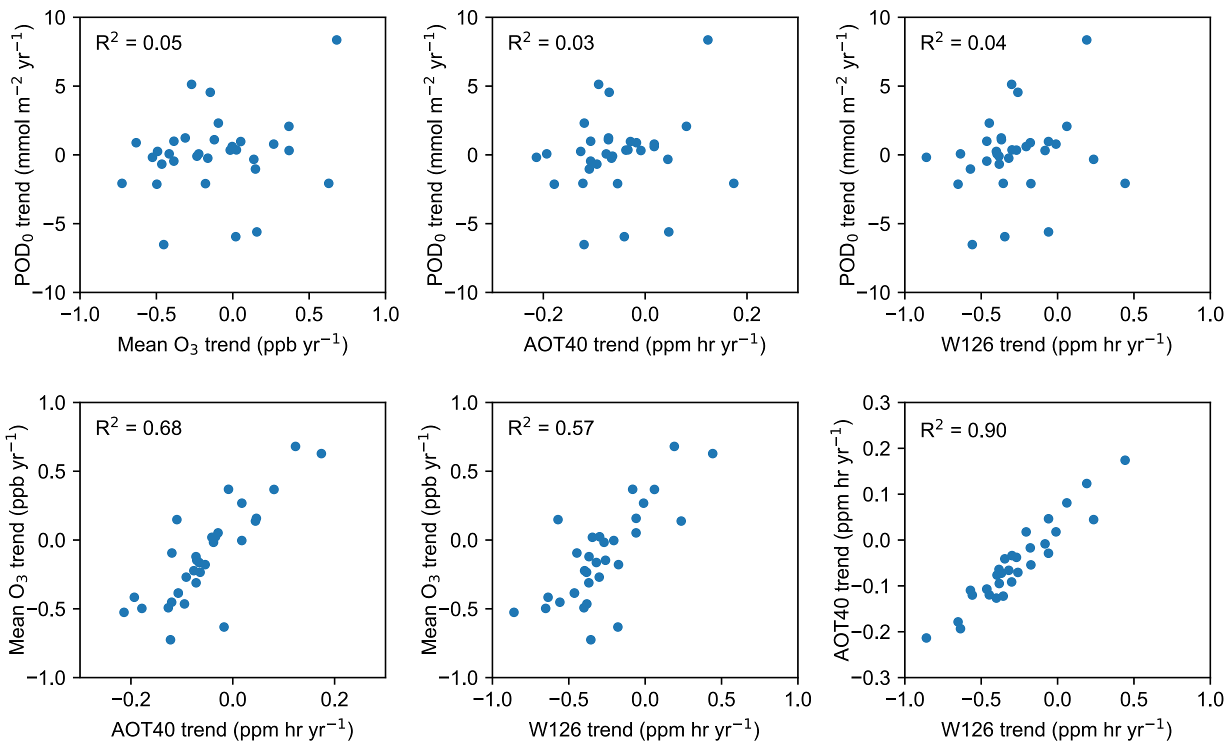

Figure 4. Co-variation of temporal trends in ozone metrics relevant to vegetation health. Each point represents fitted trends at a single site.

Supplemental material

Have improvements in ozone air quality reduced ozone uptake into plants?

Allison C. Ronan[a], Jason A. Ducker[a], Jordan L. Schnell[b], Christopher D. Holmes[a*]

[a]*Department of Earth, Ocean, and Atmospheric Science, Florida State University, Tallahassee, Florida, USA*

[b]*Department of Earth and Planetary Sciences, Northwestern University, Evanston, Illinois, USA*

*Corresponding author: cdholmes@fsu.edu

List of Contents:

Table S1. SynFlux sites used in this work and their O_3 trends. All are Tier 1 in FLUXNET2015.

Site ID	PFT[1]	O_3 Trend, % yr^{-1}				Site Name
		Mean	AOT40	W126	POD_0	
AT-Neu	GRA	–1.3	–6.7	–7.8	–1.3	Neustift
BE-Bra	MF	–0.4	–6.6	–8.6	3.1	Brasschaat
BE-Vie	MF	–1.0	–6.6	–8.6	2.1	Vielsalm
CH-Cha	GRA	0.1	–2.0	–4.9	–6.8	Chamau
CH-Dav	ENF	0.1	–1.7	–4.4	0.8	Davos
CH-Lae	MF	0.0	–1.8	–3.9	0.2	Laegern
CZ-wet	WET	–1.2	–6.3	–9.2	–9.5	Trevon (CZECHWET)
DE-Gri	GRA	–1.1	–6.3	–8.1	3.0	Grillenburg
DE-Tha	ENF	–1.1	–6.3	–8.1	–1.6	Tharandt
DK-Sor	DBF	0.2	–6.7	–3.9	1.1	Soroe
FI-Hyy	ENF	–2.3	–4.7	–13.5	3.4	Hyytiala
FR-Fon	DBF	–0.4	–6.0	–6.7	5.9	Fontainebleau-Barbeau
FR-Gri	GRA	–0.9	–8.6	–8.4	9.9	Grignon
FR-Pue	EBF	–0.6	–2.5	–5.2	–0.7	Puechabon
IT-BCi	CRO	–0.2	–4.3	–7.2	6.1	Borgo Cioffi
IT-Co1	DBF	0.4	–4.1	–8.7	–2.5	Collelongo
IT-Lav	ENF	1.0	3.6	0.9	3.2	Lavarone
IT-MBo	GRA	1.8	5.7	2.8	8.7	Monte Bondone
IT-Noe	CSH	–1.0	–8.7	–11.6	0.8	Arca di Noe – Le Prigionette
IT-Ren	ENF	0.4	2.9	–1.1	–9.2	Renon
NL-Loo	ENF	–0.7	–6.4	–8.4	0.1	Loobos
RU-Fyo	ENF	0.9	6.0	–0.8	1.5	Fyodorovskoye
US-GLE	ENF	–0.4	–1.4	–1.7	–7.4	GLEES
US-MMS	DBF	–1.2	–6.2	–7.5	–4.1	Morgan Monroe State Forest
US-Me2	ENF	1.1	–1.1	–4.0	2.0	Metolius mature ponderosa pine
US-NR1	ENF	0.0	0.4	–1.6	2.0	Niwot Ridge Forest (LTER NWT1)
US-Ne2	CRO	1.7	9.8	8.6	–3.7	Mead – irrigated maize-soybean rotations site
US-PFa	MF	–2.2	–13.5	–11.6	–5.0	Park Falls/WLEF
US-SRM	WSA	–0.4	–2.3	–3.6	–4.2	Santa Rita Mesquite
US-Ton	WSA	–1.1	–4.8	–7.7	–3.1	Tonzi Ranch
US-UMB	DBF	–1.5	–10.5	–10.0	0.6	University of Michigan Biological Station
US-UMd	DBF	0.3	2.0	3.9	–0.6	UMBS Disturbance

[1] Plant functional type. CRO: crop, CSH: closed shrubland, DBF: deciduous broadleaf forest, EBF: evergreen broadleaf forest, ENF: evergreen needleleaf forest, GRA: grassland, MF: mixed forest, WET: wetland, WSA: woody savanna.

Table S2. Temporal correlation (R^2) between O_3 flux and concentration metrics[a]

Metrics	Pooled[b]	Site-by-site[c]	Trends[d]
mean O_3 & AOT40	0.83 ± 0.02	0.80 ± 0.05	$0.68\,^{+0.09}_{-0.11}$
mean O_3 & W126	0.70 ± 0.03	0.72 ± 0.04	$0.57\,^{+0.11}_{-0.13}$
AOT40 & W126	0.88 ± 0.01	0.84 ± 0.04	$0.90\,^{+0.03}_{-0.04}$
POD_0 & mean O_3	< 0.01	0.14 ± 0.03	$0.05\,^{+0.10}_{-0.05}$
POD_0 & AOT40	< 0.01	0.12 ± 0.03	$0.03\,^{+0.09}_{-0.02}$
POD_0 & W126	< 0.01	0.14 ± 0.03	$0.04\,^{+0.10}_{-0.04}$
POD_3 & mean O_3	< 0.01	0.20 ± 0.04	$0.08\,^{+0.11}_{-0.07}$
POD_3 & AOT40	< 0.01	0.19 ± 0.04	$0.06\,^{+0.11}_{-0.06}$
POD_3 & W126	< 0.01	0.22 ± 0.04	$0.05\,^{+0.10}_{-0.05}$

[a] Values in table are the coefficients of determination. Underlying metrics are for summer daytime 2005-2014.

[b] Correlation of all metric anomalies, which have no mean spatial differences, pooled across sites and years (n = 299). See also Figures 3, S2.

[c] Correlation calculated at each site (m = 8-10 years), then the R^2 values are averaged across sites (n = 32). Range is the multi-site standard error.

[d] Correlation of temporal trends (i.e. regression slopes; n = 32 sites). See also Figures 4, S3.

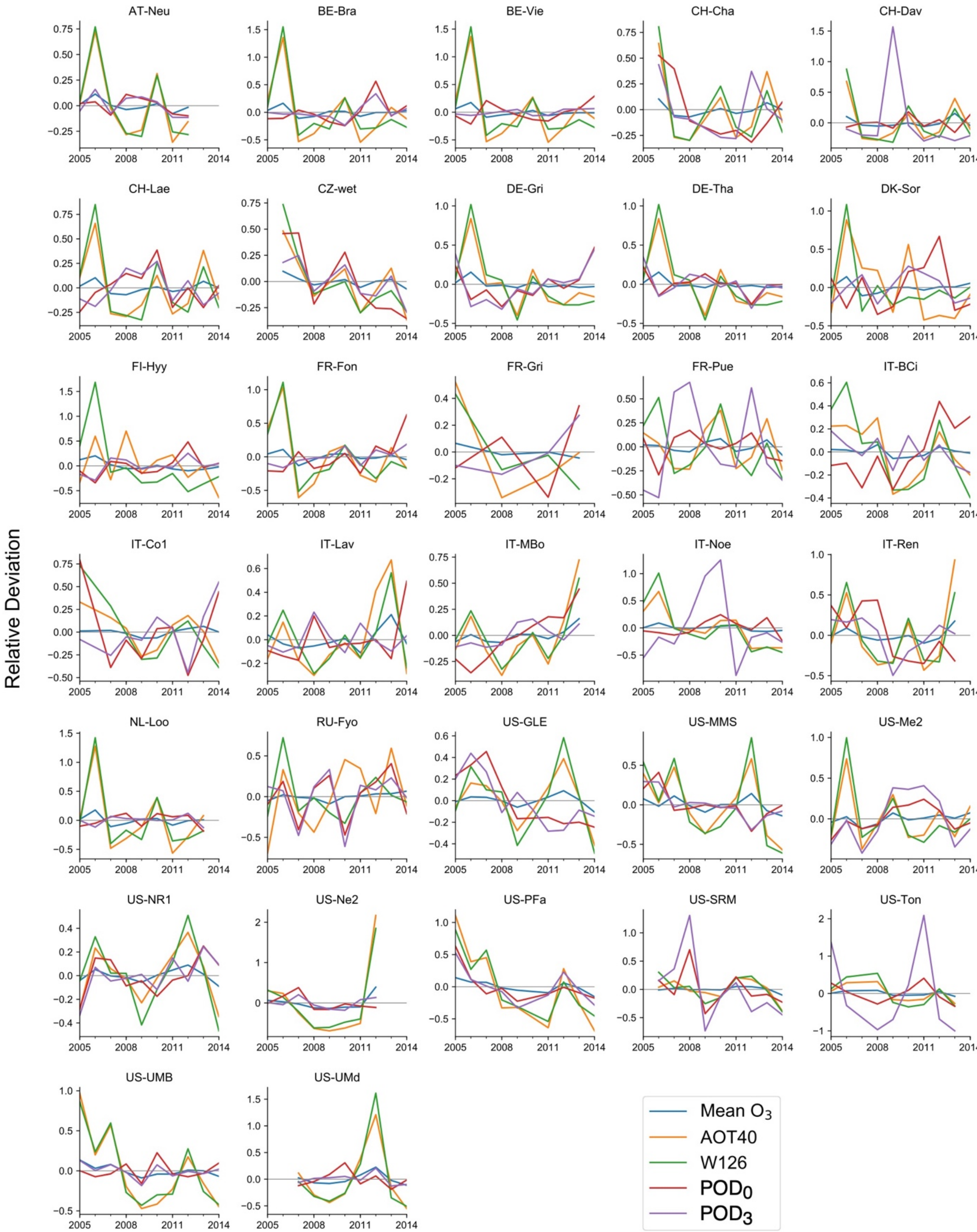

Figure S1. Time series (2005-2014) of ozone flux and concentration at all sites. Values are shown as relative deviation from the ten-year mean of each metric at each site (value/mean – 1).

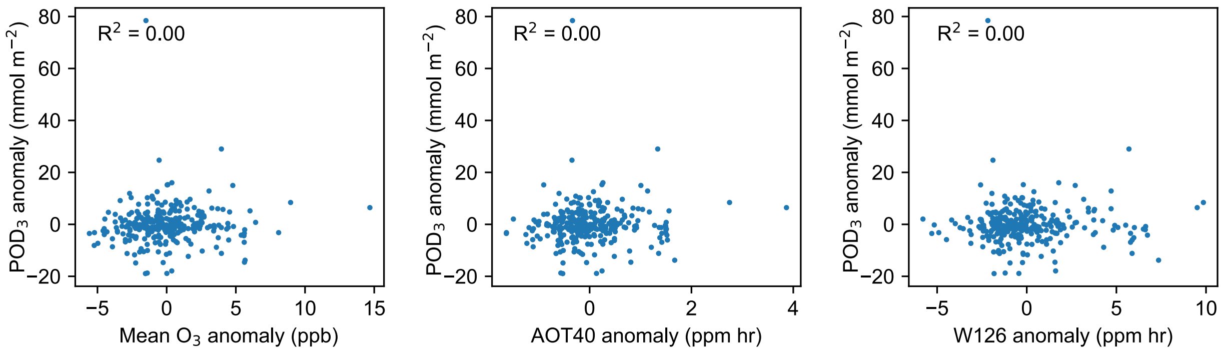

Figure S2. Temporal co-variation of POD_3 with concentration metrics. As in Figure 3, each point represents a single site and year. The site-specific mean has been subtracted from each metric to highlight temporal co-variability.

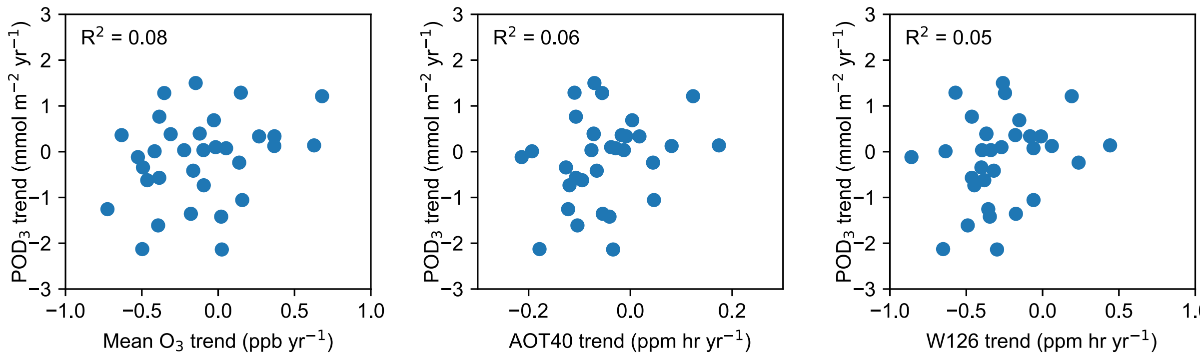

Figure S3. Co-variation of temporal trends in POD_3 and concentration metrics. As in Figure 4, each point represents fitted trends at a single site.